Infrared multiphoton dissociation of styrene ions by lowpower continuous CO2 laser irradiation

Robert C. Dunbar and Rebecca C. Zaniewski

Citation: The Journal of Chemical Physics **96**, 5069 (1992); doi: 10.1063/1.462860
View online: http://dx.doi.org/10.1063/1.462860
View Table of Contents: http://scitation.aip.org/content/aip/journal/jcp/96/7?ver=pdfcov
Published by the AIP Publishing

Infrared multiphoton dissociation of styrene ions by low-power continuous CO_2 laser irradiation

Robert C. Dunbar[a] and Rebecca C. Zaniewski
Chemistry Department, Case Western Reserve University, Cleveland, Ohio 44106

(Received 15 November 1991; accepted 9 December 1991)

The kinetics of infrared multiphoton dissociation of styrene ions under collision-free conditions in the ion cyclotron resonance ion trap were studied as a function of the intensity of the cw CO_2 laser at powers up to 6 W. Following the beginning of irradiation an induction time was observed, followed by dissociation according to a first-order rate constant. The kinetics could be fitted to a random-walk simulation of a master-equation model, in the same way as previous studies. A matrix-algebra solution of the master-equation model is described which gave a better fit with greater computational convenience. From the modeling the rate of radiation of infrared photons (assumed to be at 940 cm^{-1}) from the ions was estimated as 350 s^{-1} at an ion internal energy of around 3 eV. When the dissociation threshold E_t was treated as an unknown it was found that master-equation modeling of the kinetic results could give an estimate of E_t, but with large uncertainty. Application of simple thermal kinetic theory via Tolman's theorem gave good qualitative understanding of the results, and predicted the intensity dependence of the dissociation rate with a deviation of about 30%.

INTRODUCTION

The decomposition of gas-phase molecules by infrared multiphoton decomposition (IRMPD) using high-power pulsed lasers has been the subject of much interest and study;[1] but when this is done with a low-power, continuous-wave infrared laser the chemistry and kinetics have unique features which have been less well explored.[2-4] Two aspects have particular current interest: low-power IRMPD seems to be an excellent way to dissociate an ion selectively along its lowest-energy dissociation pathway;[5] and various approaches involving low-power IRMPD are being pursued as possible routes to IR spectroscopy of gas-phase ions.[6,7] Both of these aspects of IRMPD behavior are interesting for their capability of distinguishing isomeric ions.

As described in the previous papers in this series,[8,9] we have tried to expand our understanding of IRMPD chemistry for the particularly convenient case of gas-phase ions contained in the ion cyclotron resonance (ICR) ion trap. A first publication setting out some theoretical perspectives[8] was followed by a second paper describing a detailed study of IRMPD of *n*-butylbenzene ions.[9] Our application of straightforward master-equation modeling to the kinetics of the *n*-butylbenzene case was successful, and we regarded this as the first clear encouragement that low-intensity IRMPD kinetics may show a useful degree of regularity and simplicity, at least in the case of larger ions.

The first goal of the present study was to show that this was not an isolated success, but that the same type of approach and analysis would be similarly successful in modeling and understanding another quite different ion dissociation. We also wanted to explore further the possibility of extracting useful quantitative thermochemical information from the IRMPD kinetic results. In the course of this, it was found to be valuable to use a matrix-algebra solution of the master-equation formulation of the kinetics, and this formalism is laid out here in some detail. Finally, the modeling of this system leads to a good quantitative understanding of the excitation and relaxation processes governing the styrene ion IRMPD kinetics.

The unimolecular decomposition of styrene ion contrasts with *n*-butylbenzene ion. In addition to being smaller (42 vs 66 internal degrees of freedom), it has a rather high effective dissociation threshold[10] ($\sim$3.0 eV) as opposed to the low threshold for butylbenzene ion ($\sim$1.2 eV). These two factors mean that in the styrene ion case the internal temperature is very high at the dissociation threshold, so that one expects the radiative cooling rate to be fast at threshold. It requires accumulation of approximately 25 IR photons, in competition with rapid radiative cooling, to achieve IRMPD of the styrene ion. The weak bond strength and larger size of *n*-butylbenzene ion put it at the opposite extreme, such that only about 9 IR photons need to be accumulated in competition with relatively feeble radiative cooling to achieve dissociation. One expected consequence of this is that it should require much more vigorous IR pumping to dissociate the styrene ion, and indeed focusing of the IR laser beam was needed to achieve the modest dissociation rates reported here, corresponding to substantially higher intensity than was needed in the *n*-butylbenzene case.

EXPERIMENT

The experiments reported here used methods quite similar to those described in the butylbenzene ion IRMPD study.[9] Ions were produced by electron impact in the cell of the Fourier-transform (FT) ICR spectrometer. They were trapped for a period of 1 s to allow radiative temperature equilibration with the cell walls. An ion ejection pulse was applied to remove any m/z 78 ions present before IR irradiation. Then the IR laser was turned on for a variable time t. At the end of IR irradiation the extent of conversion of styrene

[a] Author to whom correspondence should be addressed.

 0021-9606/92/075069-07$06.00

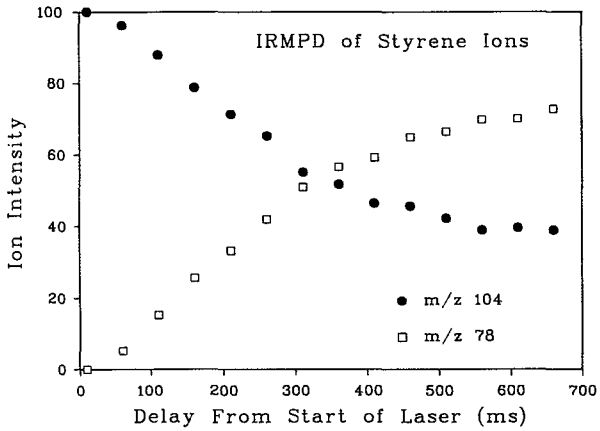

FIG. 1. Observed evolution of parent ion (m/z 104) and photofragment ion (m/z 78) populations as a function of laser irradiation time. The CO_2 laser was turned on at zero time, with an intensity in this case of 5.98 W.

parent ions to m/z 78 daughter ions was determined by FT-ICR detection.

The laser was a homebuilt CO_2 laser capable of delivering up to about 10 W at 940 cm^{-1}. The beam was focused with a concave mirror of about 1.2 m focal length, and illuminated the ions perpendicular to the magnetic-field direction. The focus was not sharp, since the spherical mirror was not illuminated at normal incidence (actually about 30° away from normal), so that vertical and horizontal focal points were substantially separated. We did not attempt a meaningful estimate of the beam size at the position of the ion cloud. It should be noted that the combination of magnetron circulation in the x-y plane and oscillation of the ions along the z axis results in extensive averaging of the position of any individual ion in the ion cloud on a time scale less than 1 ms,[11] which is faster than any time scale relevant to these kinetics. Therefore, even though the laser beam was probably smaller than the ion cloud, it could be hoped that the effective illumination of the ions would be reasonably uniform averaged over the relevant time scales.

However, it appeared that a fraction of the ions in the cloud were not well illuminated, and a residue of about 35% of the initial parent-ion population persisted at very long times. The parent-ion decay was reasonably exponential, approaching this limit of 65% dissociation asymptotically. (Fig. 1 shows a typical decay curve.) Accordingly, we treated the data on the approximation that 65% of the ion cloud was uniformly illuminated and dissociated by simple first-order kinetics, while 35% of the ions were effectively in the dark and did not dissociate at all. This gave reasonably good fits to the observed curves, and led to the rate constants k_{diss} reported below derived from the decay time constant of the dissociative fraction of the ion population.

Indicated cell pressures were around 1×10^{-8} Torr, corresponding roughly to a collision rate of 0.3 s^{-1}. Even with the worst-case assumption that every collision results in complete ion relaxation, collisional relaxation is completely insignificant compared with the dissociation and radiative relaxation rates at all laser intensities used, and it seemed entirely justified to treat the kinetics in the collision-free limit.

RESULTS

Experimental results

The lowest energy dissociation of the styrene ion is well known,

$$C_8H_8^+ \rightarrow C_6H_6^+ + C_2H_2. \quad (1)$$

The endothermicity (zero Kelvin) of this process is 2.42 eV,[10] but its rate rises relatively slowly with energy, and the threshold for dissociation at observable rates is closer to 3 eV. This was the only reaction observed in IRMPD.

Six curves for dissociation vs time were measured over a range of laser intensities from 2.85 to 6 W. Each curve was plotted as $\ln(f)$ vs t, where f is the fraction of parent ions remaining. The slope was taken at long τ (actually at the point where 30% of the illuminated parent ions were dissociated) and assigned as k_{diss}. The tangent to the curve was extended back to the intercept with the $f=1$ line, and the value of τ at this point was assigned as the induction time τ_{ind}. These results are given in Table I.

Random-walk computer simulation

Further analysis of these results depends on fitting to computer-simulated kinetics. The initial analysis was done using a random-walk simulation as was described for the n-butylbenzene case.[8,9] Values were assigned for the photon absorption rate, stimulated emission rate, and spontaneous emission rate as a function of internal energy of the styrene ion. Starting with the ion at 0.17 eV (375 K), the ion was allowed to move randomly up and down the internal energy axis until it exceeded the assumed dissociation threshold at 3.0 eV. For each simulated laser intensity I_{rw} the simulation yielded simulated values of the dissociation rate constant, k_{rw}, and the induction time, τ_{rw}.

The "sudden death" assumption was made, that when the internal energy of an ion exceeds a threshold E_t, it dissociates rapidly compared with all other processes, but it does not dissociate below E_t. E_t is roughly the internal energy at which the unimolecular dissociation rate of the ion becomes greater than the relaxation rate k_{rel}. Assuming the relaxation rate to be of the order of 10^2, the known rate-energy curve of the styrene ion[9] can be extrapolated to give an estimate of 3.0 eV for E_t.

A laser photon energy of 940 cm^{-1} was used. An energy

TABLE I. Experimental results.

I_{laser} (W)	k_{diss} (s^{-1})	τ_{diss} (s)
6.0	5.66	0.073
5.05	2.65	0.095
4.0	0.95	0.140
4.0	0.74	0.125
2.95	0.166	0.225
2.85	0.103	0.200

of 800 cm^{-1} was assigned as the typical energy of an emitted IR photon, based on the following considerations. In the mid-infrared region, the infrared absorption spectrum of neutral styrene is dominated by several very intense absorptions in the 700–900 cm^{-1} region. At moderate internal temperatures (up to perhaps 1000 K, corresponding to an ion internal energy of about 1.5 eV) these are likely to be the only significant radiative cooling modes, and the assumption of an average effective radiative frequency around 800 cm^{-1} is sound. At higher energies the C–H stretches around 3000 cm^{-1} may come into play, depending on their relative absorption strengths relative to the lower-frequency modes, which are not well known. As a suggestion of how significant these modes might be, it was calculated that at the internal energy of the dissociation threshold (3 eV, or 1550 K internal temperature), and assuming *equal oscillator strengths* at 800 and at 3000 cm^{-1}, the rates of IR photon emission would be equal for 800 and 3000 cm^{-1} modes. However, we do not know these oscillator strengths for the ion, so no truly meaningful numbers can be assigned. In the face of this uncertainty, we decided to ignore any possible contribution from the C–H stretches, and take the radiating photon energy to be 800 cm^{-1} over the entire range of ion internal energies. Modeling using substantial contributions from C–H stretching-mode radiation gave fits to the data which were worse, but not drastically worse, than the fit described here.

Fitting simulated and experimental values followed the same plan as before.[9] Three unknown parameters connect the observed and simulated experiments: Two constants relate the experimental laser intensity I_{laser} and the simulated intensity I_{rw}, according to

$$I_{rw} = B(I_{\text{wall}} + I_{\text{laser}}), \tag{2}$$

where I_{wall} represents the (unknown) equivalent light intensity illuminating the ions from the cell walls in the absence of CO_2 laser irradiation, and B is a proportionality constant. The third unknown parameter is the constant R giving the time in seconds corresponding to one time step in the computer random walk.

The constant BI_{wall} was evaluated by assuming that with the CO_2 laser off the ions equilibrated to a temperature of 375 K. The value of I_{rw} giving this equilibrium ion temperature was determined from the simulation program, and was set equal to BI_{wall}. The constant B was found through calculating the dimensionless ratio $W = \tau_{rw} k_{rw}$ (or $\tau_{\text{ind}} k_{\text{diss}}$ for the experimental points). W values were calculated as a function of I_{laser} for the experimental points, and also as a function of I_{rw} for the simulated points. Comparison of these two sets of W calculations with each other as described before[9] gave a quite closely constrained value of B. Finally, the value of R came directly from a comparison of the observed and the simulated decay curves at a given value of I_{laser} and the corresponding value of I_{rw}.

The fit resulting from this fitting procedure is shown in Figs. 2 and 3, plotting the experimentally observed values of k_{diss} and τ_{ind} along with the fitted curves from the simulations. The fit is reasonable, except that the dissociation rate is underestimated at high intensities.

As was discussed in detail in the earlier papers,[8,9] an internal temperature for the ions can be defined as a function of the irradiating laser intensity. Once we have established the correspondence between the simulated and experimental laser intensities, it is straightforward to calculate this steady-state temperature with the simulation program, and then assign the temperatures corresponding to the experimental laser intensities. This temperature scale is tabulated in Table II.

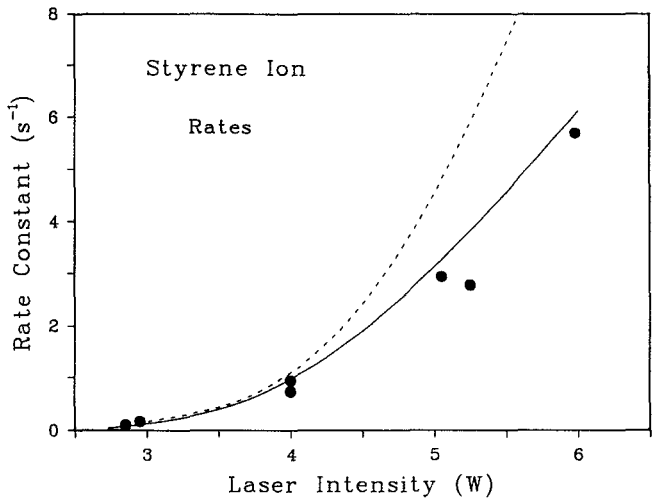

FIG. 2. Experimental values of the rate constant k_{diss} compared with predictions from the simulation fits. The dashed curve is from the random-walk simulation, and the solid curve is from the matrix solution of the master equation.

Matrix solution of the master equation

The random-walk simulations described above to model the IRMPD kinetics provide one way to solve the master equation numerically. An alternative approach, the direct solution of the master equation by matrix algebra,[12,13] has

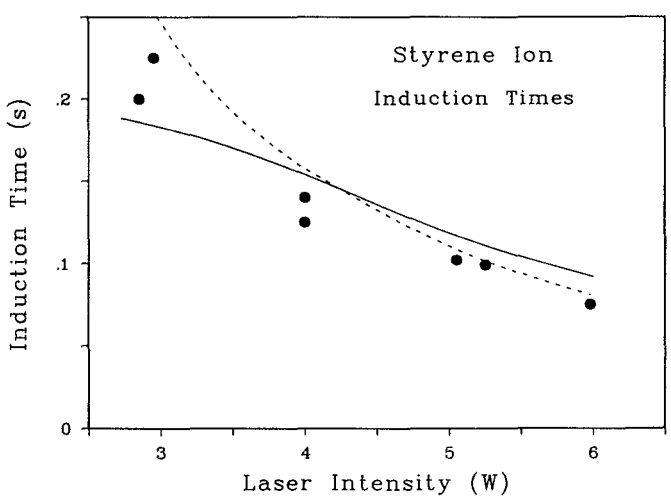

FIG. 3. Experimental values of the induction time τ_{ind} compared with predictions from the simulation fits. The dashed curve is the random-walk simulation, and the solid curve is the matrix solution of the master equation.

TABLE II. Modeled internal temperatures of the styrene ion population under laser irradiation assuming no dissociation.

Intensity (W)	Temperature (K)	Internal energy $\langle E \rangle$ (eV)
0	375	0.17
1	610	0.54
2	795	0.94
3	960	1.35
4	1120	1.78
5	1280	2.23
6	1440	2.71

some important advantages, and is carried through in this section. The random-walk approach used above is attractive because it provides a convincing, physically rooted picture of the kinetics without the intervention of much formal mathematics, and because it is highly flexible in terms of the physical models which can be treated. On the other hand, advantages of the matrix solution are that it is free of uncertainty from statistical fluctuations; and that once the apparatus is set up, it is convenient to generate solutions for a wide range of models and parameters.

The ion population is described by the occupations N_i of the set of energy levels. In this work, a ladder of energy levels was used which were equally spaced in energy with a spacing of 470 cm^{-1}, which is half the energy of the CO_2 laser photon. The population at any time t is characterized by the occupation vector $\mathbf{N}(t)$, whose elements are N_i. The observable quantity is $C(t)$, the total ion population, which is the sum of the N_i's. The occupation vector is normalized such that $C(t) = \Sigma_i N_i = 1$ at $t = 0$, but $C(t)$ will decrease below unity at later times as some of the ions react (dissociate). The transport matrix J is defined to describe the evolution of the population according to a master equation in the form

$$d\mathbf{N}/dt = -\mathsf{J}\cdot\mathbf{N} \tag{3}$$

(which is a coupled set of differential equations). In the styrene ion simulations discussed here, the nonzero elements of the transport matrix were taken as

$$J_{ii} = \begin{cases} Ik_{\mathrm{up};i\to i+2} & (i = 1,2), \\ Ik_{\mathrm{up};i\to i+2} + Ik_{\mathrm{dn};i\to i-2} + k_{\mathrm{rad};i\to i-2} & \\ \quad (i \text{ from 3 to thr}), & \\ k_{\mathrm{loss}} \quad (i > \mathrm{thr}), & \end{cases} \tag{4}$$

$$J_{i,i+2} = -Ik_{\mathrm{dn};i\to i-2} - k_{\mathrm{rad};i\to i-2},$$

$$J_{i,i-2} = -Ik_{\mathrm{up};i\to i+2} \quad (i \geqslant 3),$$

where $k_{\mathrm{up}} = k_{\mathrm{dn}}$ are the rate constants for absorption and induced emission of laser photons, I is the laser intensity, k_{rad} is the rate constant for spontaneous emission of an infrared photon, and thr is the threshold energy level above which the ion is assumed to dissociate with a large rate k_{loss}. The rate constants used in the J matrix were calculated in the same way as the corresponding rate constants described above for the random-walk simulation.

For comparison with experiment we want to calculate the rate constant k_∞ for ion disappearance in the limit of long time, and τ_∞, the corresponding induction time (see Fig. 4). If we diagonalize J to get its eigenvalues λ_i and its eigenvectors $\mathbf{B}^i$, it is well known that the lowest eigenvalue, λ_0, is the limiting rate constant,

$$k_\infty = \lambda_0, \tag{5}$$

and the corresponding eigenvector $\mathbf{B}^0$ describes the long-time (decaying) steady-state population distribution.

Let us describe the initial state of the population, $N(0)$, with an expansion in terms of the eigenvectors,

$$\mathbf{N}(0) = \sum_j c_j \mathbf{B}^j = \mathsf{B}\cdot\mathbf{c}, \tag{6}$$

where $\mathbf{c}$ is the column vector of c_j coefficients, and B is the matrix whose columns are the eigenvectors of J. The coefficients c_j are found by multiplying this equation on the left by B^{-1},

$$\mathbf{c} = \mathsf{B}^{-1}\cdot\mathbf{N}(0). \tag{7}$$

Then the evolution of the population can be explicitly written in the form

$$C(t) = \sum_i \left(\sum_j \mathbf{B}_j^i \right) c_i e^{-\lambda_i t} = \mathbf{u}\cdot\mathsf{B}\cdot\mathsf{M}\cdot\mathbf{c}, \tag{8}$$

where $\mathbf{u}$ is the row vector with all elements of unity, and M is a diagonal matrix whose diagonal elements are $e^{-\lambda_i t}$. The induction time τ_∞ is quickly written as follows from the construction of Fig. 4 and from Eq. (8):

$$\exp[-\lambda_0 (t_{\mathrm{long}} - \tau_\infty)] = C(t_{\mathrm{long}}), \tag{9}$$

where t_{long} is a time long enough that all of the higher components of the expansion in Eq. (8) have died away compared with the λ_0 component. In the long-time limit we have

$$C(t_{\mathrm{long}}) = c_0 \exp(-\lambda_0 t_{\mathrm{long}}) \sum_i \mathbf{B}_i^0, \tag{10}$$

which gives

$$\tau_\infty = -(1/\lambda_0) \ln\left(c_0 \sum_i \mathbf{B}_i^0 \right). \tag{11}$$

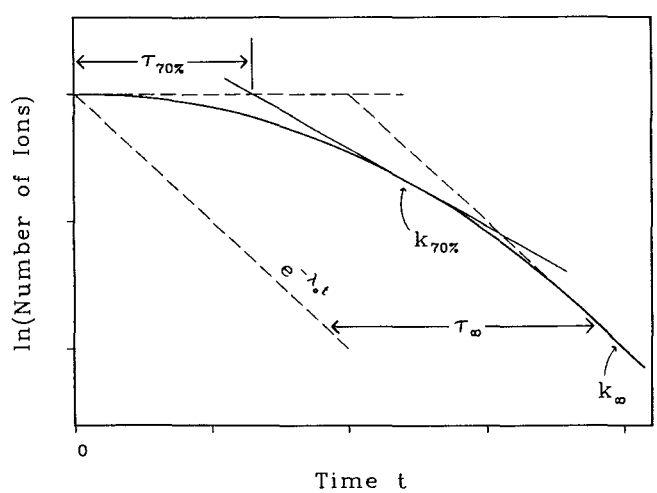

FIG. 4. Schematic diagram of the parent-ion decay curve (solid line), showing the various quantities defined and discussed in the text.

At low laser intensities where dissociation is negligible, the lowest eigenvector $\mathbf{B}^0$ gives the steady-state distribution. The average energy of the steady-state population is then given by

$$\langle E \rangle = \sum_i \epsilon_i \mathbf{B}_i^0 / \sum_i \mathbf{B}_i^0. \tag{12}$$

where ϵ_i is the energy of the ith energy level. By finding the irradiation intensity I_{thermal} which makes $\langle E \rangle$ equal to the room-temperature energy of styrene ions, the thermal light intensity correction is precisely and conveniently available.

In practice, these simple explicit expressions for k_∞ and τ_∞ are not quite appropriate for comparison with our experimental curves, because the long-time limiting values cannot be extracted from real data. This is particularly true at high intensities, where the ln $C(t)$ vs t curves still show marked curvature at the longest times at which ions can still be observed. It is convenient in practice to look at the slopes of the ln $C(t)$ vs t curves at an arbitrary but standardized point in time, say the point at which 70% of the initial ion population still remains. As illustrated in Fig. 4, the rate constant $k_{70\%}$ is measured as the slope of the curve at that point, and the induction time $\tau_{70\%}$ is the apparent induction time based on the tangent line at that point. These practical values are readily simulated within the master-equation formalism as follows.

First, using Eq. (11), the time $t_{70\%}$ is found at which $C(t_{70\%}) = 0.7$. Then the slope $d \ln C(t)/dt$ comes from Eq. (8),

$$d \ln C(t)/dt = [1/C(t)] \sum_i c_i \lambda_i e^{-\lambda_i t} \left(\sum_j \mathbf{B}_j^i \right) \tag{13}$$

and

$$k_{70\%} = [-d \ln C(t)/dt]_{t = t_{70\%}}. \tag{14}$$

The induction time $\tau_{70\%}$ is the intercept at ln $C(t) = 0$ of the tangent line through the 70% point (as in Fig. 4), and is immediately found to be

$$\tau_{70\%} = t_{70\%} + \ln(0.7)/k_{70\%}. \tag{15}$$

It is straightforward for the computer to set up the transport matrix J and carry through the steps to give $k_{70\%}$ and $\tau_{70\%}$ as a function of the laser intensity I, the rate parameters k_{up} and k_{rel}, and the threshold value thr.

In the present simulations, the threshold was again taken as 3.0 eV (thr = 52). From Eq. (12) the thermal radiation contribution BI_{wall} [Eq. (2)] of 0.05 was calculated corresponding to a temperature of 375 K for the ion population, and BI_{wall} was added to the simulated laser intensity. For each given set of values of Ik_{up} and k_{rel} three quantities were calculated for comparison with experiment: the rate constant $k_{70\%}$; the induction time $\tau_{70\%}$; and Δ, the derivative of the rate constant with respect to the intensity, $\Delta = d \ln k_{70\%}/d \ln I$. The fit of these simulated results to the experimental values might be carried through in precisely the same way as was described above for the random-walk approach. However, the more facile calculations in the matrix formulation make it feasible to fit by a more direct and accurate procedure, in which the simulation parameters are varied systematically to find the minimum of an appropriate least-squares quantity (called χ in the following) which quantifies the deviation between experiment and simulation. Such a least-squares minimization is briefly outlined below.

The experimental results can be smoothed and conveniently summarized by three values (measured near the middle of the intensity range): the dissociation rate, $k_{70\%}$, the induction time, $\tau_{70\%}$, and the slope of the rate curve, $\Delta = d \ln k / d \ln I$. The three computed numbers $k_{70\%}$, $\tau_{70\%}$, and Δ were compared with the observed values at the chosen value of the experimental laser intensity, and a deviation parameter χ was calculated according to

$$\chi = [((k_{\text{obs}} - k_{\text{calc}})/k_{\text{obs}})^2 + ((\tau_{\text{obs}} - \tau_{\text{calc}})/\tau_{\text{obs}})^2 + ((\Delta_{\text{obs}} - \Delta_{\text{calc}})/\Delta_{\text{obs}})^2]^{1/2}. \tag{16}$$

This deviation was minimized to find the best fit to experiment. This procedure was carried out for a point near the middle of the range of experimental data ($I_{\text{expt}} = 4.13$, $k_{70\%,\text{expt}} = 1.0\ \text{s}^{-1}$, $\tau_{70\%,\text{expt}} = 0.127$ s, $\Delta_{\text{expt}} = d \ln k_{70\%,\text{expt}}/d \ln I_{\text{expt}} = 5.22$ from the smoothed experimental data). The best fit to this point gave an acceptably low value of the deviation parameter χ of 0.08, indicating that the three experimental parameters were fitted with an average deviation of less than 5%. The rates and induction times calculated for this fit are compared with experiment in Figs. 2 and 3. It can be seen that the fit is substantially improved over that from the random-walk simulations, and is quite satisfactory within the uncertainties of the data and the kinetic modeling. (The improved agreement is not mainly due to any inherent difference in these two approaches, but rather to the more realistic modeling done in the matrix formulation using the 70% points instead of the infinite-time points that were used in the random-walk modeling. As expected, the two approaches to solving the master equation gave similar results in direct comparisons.)

DISCUSSION AND CONCLUSIONS

Threshold determination

One of the motivations for working through the matrix solution of the master equation for this problem was to see how closely the experimental data can be used to pin down the threshold energy. In the analysis described above, two undetermined parameters of the kinetic model, Ik_{up} and k_{rel}, were fixed by comparing the simulation with three independent experimental values, k, τ, and Δ. It should be possible to fix a third undetermined parameter from the three experimental observables, and we set out to see if the threshold E_t could be treated as an unknown and determined by fitting to the experimental values. The matrix analysis of the master equation was carried out as described above for a series of assumed values of E_t, with the deviation parameter χ being minimized in each case.

Figure 5 shows the variation of the best-fit value of χ as a function of the assumed threshold energy. The assumed value of the threshold giving the best fit to the data is about 2.7 eV, from the minimum of this curve. We consider, somewhat arbitrarily, that the three experimental numbers, k, τ, and Δ, are each uncertain to about 10%. Assuming that these uncertainties are statistically independent, we then expect a

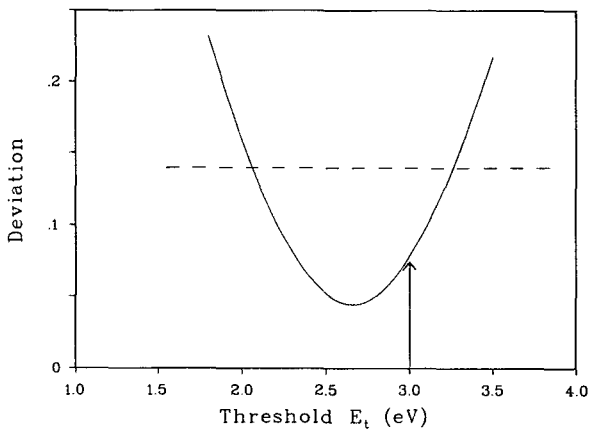

FIG. 5. The deviation χ between experiment and master-equation simulation, taking the threshold E_t as an unknown. The (assumed) true value of E_t of 3.0 eV is noted. The horizontal line at $\chi = 0.14$ is an estimate of the maximum χ value corresponding to a reasonable fit of experiment and simulation, which was used to estimate the value of E_t as 2.7 ± 0.6 eV.

maximum value of χ of $0.1\sqrt{2} = 0.14$, and we take the range of acceptable threshold energies to be the range over which χ is less than this value. This leads to an estimation of the threshold as 2.7 ± 0.6 eV. The best estimate of the threshold determined in this way is lower than the 3.0 eV derived from the rate-energy curve, but the actual value of 3.0 eV is well within the range of uncertainty of the present analysis.

This analysis is encouraging in showing that IRMPD data can be analyzed to estimate the threshold for a dissociation of unknown thermochemistry. However, the determination is not very tightly constrained or very accurate, and it appears that this approach will not yield very precise threshold values. We have seen that this threshold determination requires all three of the experimental quantities, the rate, the induction time, and the intensity dependence of the rate. The value of the threshold cannot even be estimated from a determination of the rate vs intensity alone.

IR relaxation rate

The IRMPD experiment, as fitted to the master-equation kinetic model, can be considered as a measurement of the rate of infrared radiative relaxation of the ions. Since the results are primarily sensitive to the relaxation rate in the vicinity of the dissociation threshold, the most meaningful value to quote is the relaxation rate k_{rad} at the 3.0 eV threshold energy. This value is immediately obtained from the radiative contribution to the diagonal matrix element of the J matrix at the threshold energy level. For styrene, the present analysis gives us an estimate of the radiative relaxation rate of 350 photons s^{-1} for ions near threshold.

This rate of photon emission is quite fast, in part because of the high threshold and the corresponding high temperature of near-threshold ions. Converted to a time constant for radiative cooling, this photon emission rate leads to a spontaneous radiative time constant of 73 ms, or a first-order rate constant for radiative energy loss of 13 s^{-1} at an internal energy of 3.0 eV. Interestingly, this is virtually the same as the radiative cooling rate constant (15 s^{-1}) that was determined for a benzene ion by chopped-laser methods at an internal energy of about 2.6 eV.[14]

The radiative cooling rate measured here is much faster than the radiative cooling rate constant of 0.65 s^{-1} for the styrene ion around 0.4 eV internal energy, as measured by time-resolved photodissociation.[15] This clearly illustrates that the radiative cooling time constant of an isolated molecule is a very strong function of the internal energy (internal temperature) at which we make the measurement, owing to the rapid freezing out of the radiating mode as the temperature goes down.[16]

The thermal kinetics picture

It is interesting to see how well the thermal formulation of dissociation kinetics describes this system. According to the thermal picture,[8] the intensity dependence of the dissociation rate is expressed as an activation energy,

$$E_a/k_B = d \ln k_{\text{diss}}/d(1/T), \tag{17}$$

where k_B is the Boltzmann constant. For the IRMPD case, it was shown[8] that E_a is given (within some approximations) by

$$E_a = qh\nu\, d \ln k_{\text{diss}}/d \ln(I_{\text{laser}} + I_{\text{wall}}), \tag{18}$$

where q is the partition function for a harmonic oscillator of frequency $h\nu$. This is somewhat more convenient than Eq. (17), since its use draws on the modeling results only for the estimation of q and I_{wall}, neither of which is very sensitive to modeling, whereas using Eq. (17) requires that T be calculated from modeling, which is quite sensitive to the chosen model. In the thermal formulation, the activation energy measured using Eq. (17) or (18) is expected to match the value calculated from an adjusted form of Tolman's theorem,

$$E_a = E_t - \langle E' \rangle + hm(q-1) - h\nu[1/\ln\alpha + 2\alpha/(1-\alpha^2)]. \tag{19}$$

Here E_t, the threshold energy, approximates the energy of the ions currently undergoing dissociation, $\langle E' \rangle$ is the average energy of the steady-state ion population under laser irradiation, and the last two terms are small corrections which correct for the fact that the energy input is by photon pumping rather than thermal collisions, and also correct to a first approximation for the depletion of energetic reactant ions by dissociation. The constant α is the ratio of ion population at E_t to population at $(E_t - h\nu)$, $h\nu$ is the IR photon

TABLE III. Parameters for the thermal kinetic analysis.

I_{laser}	4.1 W
k_{diss}	1.0 s^{-1}
$\langle E' \rangle$	1.65 eV
E_t	3.0 eV
T	1100 K
q	1.4
α	0.7
E_a	0.98 eV [experimental, Eq. (18)]
E_a	1.38 eV [Tolman's theorem, Eq. (19)]

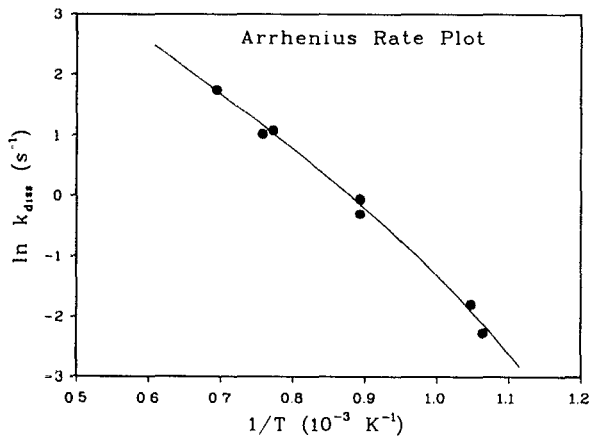

FIG. 6. Arrhenius plot of the experimental rate constants as a function of internal temperature. The temperatures were derived from the laser intensity values through the simulation described in the text. The slope of the curve is the phenomenological activation energy E_a which is compared in the text with the expectation from Tolman's theorem.

energy, and q is the partition function of a harmonic oscillator at frequency $h\nu$. We believe that this Tolman's theorem expression should become exact in the low-intensity limit where the rate of dissociation is very small compared with the excitation and relaxation processes which tend to maintain the population in a steady-state Boltzmann distribution. The interesting question is whether the present experiments approach this limit closely enough to make the thermal picture useful or illuminating.

Taking as a representative point a laser intensity of 4.1 W, near the middle of our data range, we may compare the activation energy, as measured from the slope of the rate/intensity curve, with the prediction of the thermal picture. The values of the various parameters are as shown in Table III. The experimental data are plotted in the Arrhenius form in Fig. 6.

The thermal picture is successful in giving qualitative agreement with the observed E_a, the observed activation energy (0.98 eV) being about 30% lower than predicted (1.38 eV). This is less satisfactory than the similar comparison in the n-butylbenzene ion case,[9] where the divergence between the Tolman's theorem prediction and the observed slope was only roughly 10%. The deviation from Tolman's theorem has its origin in the depletion of the upper energy levels by reaction to a greater extent than allowed for in the first-order reactive depletion correction term. The less good agreement found here somewhat dampens our hope that thermal analysis of cw IRMPD results might provide a fully quantitative approach to data analysis, and suggests that detailed master-equation modeling will probably be inescapable in the quantitative analysis of IRMPD results.

It is striking again, as it was with n-butylbenzene,[9] that the Arrhenius activation energy E_a observed for IR multiphoton activation is very much less than the reaction threshold energy, and in fact for the particular experimental point described here E_a is less than half of E_t. This illustrates again that IRMPD is an extreme case, in which a thermal kinetic picture is reasonably valid, but the activation energy E_a can only be understood through Tolman's theorem and is not even approximately equal to the reaction threshold E_t.

ACKNOWLEDGMENTS

Support is gratefully acknowledged from the National Science Foundation and from the donors of the Petroleum Research Fund, administered by the American Chemical Society. R. C. Z. was supported during this research by the Undergraduate Research Participation program of the National Science Foundation.

[1] D. W. Lupo and M. Quack, Chem. Rev. **87**, 181 (1987).
[2] L. R. Thorne and J. L. Beauchamp, in *Gas Phase Ion Chemistry*, edited by M. T. Bowers (Academic, Orlando, FL, 1984), Vol. 3; C. A. Wight and J. L. Beauchamp, Chem. Phys. **134**, 375 (1989).
[3] M. Bensimon, J. Rapin, and T. Gaumann, Int. J. Mass Spectrom. Ion Proc. **72**, 125 (1986); M. Bensimon, T. Gaumann, and G. Zhao, *ibid.* **100**, 595 (1990).
[4] K. E. Salomon and J. I. Brauman, J. Phys. Chem. **92**, 9648 (1988).
[5] M. A. Hanratty, C. M. Paulsen, and J. L. Beauchamp, J. Am. Chem. Soc. **107**, 5074 (1985); C. H. Watson, G. Baykut, M. A. Battiste, and J. R. Eyler, Anal. Chim. Acta **178**, 125 (1985); G. Baykut, C. H. Watson, R. R. Weller, and J. R. Eyler, J. Am. Chem. Soc. **107**, 8036 (1985).
[6] C. H. Watson, J. A. Zimmerman, J. E. Bruce, and J. R. Eyler, J. Phys. Chem. **95**, 6081 (1991).
[7] S. K. Shin and J. L. Beauchamp, J. Am. Chem. Soc. **112**, 2057 (1990); **112**, 2066 (1990).
[8] R. C. Dunbar, J. Chem. Phys. **95**, 2537 (1991).
[9] G. T. Uechi and R. C. Dunbar, J. Chem. Phys. (in press).
[10] R. C. Dunbar, J. Phys. Chem. **94**, 3283 (1990).
[11] R. C. Dunbar, J. H. Chen, and J. D. Hays, Int. J. Mass Spectrom. Ion Proc. **57**, 39 (1984).
[12] W. G. Valance and E. W. Schlag, J. Chem. Phys. **45**, 216 (1966).
[13] S. K. Kim, J. Chem. Phys. **28**, 1057 (1958).
[14] M. S. Ahmed, H. Y. So, and R. C. Dunbar, Chem. Phys. Lett. **151**, 128 (1988).
[15] R. C. Dunbar, J. Chem. Phys. **91**, 6080 (1989).
[16] In order to account quantitatively for the large cooling rate difference seen between 0.4 and 3 eV for the styrene ion, it seems to be necessary to assume a substantial contribution of C–H stretching mode emissions, since the emitting modes around 940 nm do not freeze out quickly enough. We will not consider this question further here, since it does not strongly affect the modeling results discussed in the present paper. As noted above, inclusion of a large oscillator strength at 3000 cm^{-1} in the emission spectrum makes the fits somewhat, but not drastically, less good than the present fits.